Colloid Polym Sci (2010) 288:189–197
DOI 10.1007/s00396-009-2152-7

ORIGINAL CONTRIBUTION

Convectional, sedimentary, and drying dissipative patterns of colloidal suspensions of polymer complexes of poly(acrylic acid) with poly(ethylene glycol) and poly(vinyl pyrrolidone)

Tsuneo Okubo · Junichi Okamoto · Akira Tsuchida

Received: 2 October 2009 / Accepted: 31 October 2009 / Published online: 25 November 2009

Abstract Convectional, sedimentary, and drying dissipative patterns were observed at room temperature on a cover glass, a watch glass, and a Petri dish during the course of dryness of aqueous suspensions of colloidal polymer complexes of poly(acrylic acid) (HPAA) with poly(ethylene glycol) (PEG) and poly(vinyl pyrrolidone) (PVP). With increase in the molecular weight of the polymer component, the complexes showed from transparent solution stable colloidal dispersion and the sticky aggregates. HPAA25K+PVP25K complex showed bluish colors and the c*olloidal crystal* suspension. Size of the macroscopic broad rings of HPAA25K+PEG decreased as molecular weight of PEG increased. Furthermore, the size increased sharply as the polymer concentration increased in the complex systems HPAA25K+PVP25K. Characteristic microscopic patterns appeared for HPAA+PEG and HPAA+PVP complexes.

Keywords Dissipative structure · Convectional pattern · Sedimentary pattern · Drying pattern · Polymer complex · Poly(acrylic acid) · Poly(ethylene glycol) · Poly(vinyl pyrrolidone) · Colloidal crystal

T. Okubo (✉)
Institute for Colloidal Organization,
Hatoyama 3-1-112, Uji,
Kyoto 611-0012, Japan
e-mail: okubotsu@ybb.ne.jp

T. Okubo
Cooperative Research Center, Yamagata University,
Johnan 4-3-16,
Yonezawa 992-8510, Japan

J. Okamoto · A. Tsuchida
Department of Applied Chemistry, Gifu University,
Yanagido 1-1,
Gifu 501-1193, Japan

Introduction

Most structural patterns in nature form via self-organization accompanied with the *dissipation* of free energy and in the nonequilibrium state. In order to understand the mechanisms of the dissipative self-organization of the simple model systems, instead of the much complex nature itself, the authors have studied the *convectional*, *sedimentary*, and *drying* dissipative patterns during the course of dryness of colloidal suspensions and solutions as systematically as possible, though the three kinds of patterns are correlated strongly and overlapped each other [1, 2].

Typical *convectional* patterns, which have been reported so far, are the *hexagonal circulating* pattern, *Benard cell* [3, 4], and the spoke lines spreading the whole liquid surface accompanied with the huge number of cell convections in the normal direction of the spoke lines, *Terada cell* [5–7]. These convectional patterns were observed often in the intermediate and final steps in the convectional processes [8–16]. Recently, the whole process of the convectional patterns has been clarified experimentally [10, 12, 13]. Theoretical studies of the convectional patterns have been made mainly using Navier–Stokes equations, but these are not always successful [17–22].

Sedimentary dissipative patterns during the course of drying suspensions have been studied in detail in a glass dish, a cover glass, a watch glass, and others, for the first time, in our laboratory [10, 23–30]. The broad ring-like patterns were formed in suspension state. It was clarified that the sedimentary particles were suspended above the substrate and always moved by the balancing of the external force fields between convectional flow and sedimentation. Quite recently, dynamic bundle-like sedimentary patterns formed cooperatively from the spoke-like convectional structures for coffee [12] and black tea [13].

Drying dissipative patterns have been studied for suspensions or solutions of many kinds of colloidal particles [8, 9, 12, 13, 23–46], linear-type synthetic and bio-polyelectrolytes [47, 48], water-soluble neutral polymers [49, 50], ionic and nonionic detergents [39, 51, 52], gels [53], and dyes [54] mainly on a cover glass. The macroscopic broad ring patterns of the hill, accumulated with the solutes in the outside edges, always formed. For the non-spherical particles, the round hill was formed in the central area in addition to the broad ring. Macroscopic spoke-like cracks or fine hills including flickering spoke-like ones were also observed for many solutes. Beautiful fractal patterns such as branch-like, arc-like, block-like, star-like, cross-like, and string-like ones were observed in the microscopic scale. One of the important findings in our experiments is that the primitive vague sedimentary patterns were formed already in the concentrated suspensions or solutions before dryness, and they grew toward fine structures in the processes of the solidification. It has been clarified that *information* of the suspensions and solutions is *transferred* into the drying patterns. Furthermore, *dissipative crystallization* of poly(allylamine hydrochloride) [47], poly (ethylene glycol) (PEG) [55], and sodium salt of poly (methacrylic acid) [56] was studied in detail.

In this work, convectional, sedimentary, and drying dissipative patterns were observed successfully for the colloidal suspensions of the hydrogen-bonding polymer complexes of poly(acrylic acid) (HPAA) with PEG and poly (vinyl pyrrolidone) (PVP). Hydrogen-bonding polymer complexes have been studied by many researchers in aqueous media [57–68]. In several systems, the affinitive interaction between the polymers is appropriately strong enough to make stable colloidal suspensions. The kinetic analyses of the polymer complexes between HPPA+PVP in the homogeneous solution state were reported by the author's group [69].

Experimental

Materials

Samples of HPAA, HPAA25K (molecular weight, MW=ca. 15,000 by the manufacturer) and HPAA250K (ca. 250,000), were used in this work. Nine samples of PEG, PEG0.2K (MW=180–220), PEG1K (ca. 1,000), PEG2K (ca. 2,000), PEG4K (ca. 3,000), PEG8K (ca. 8,000), PEG20K (20,000± 5,000), PEG500K (300,000–500,000), PEG2000K (1,500,000–2,000,000), and PEG3500 (3,000,000–3,500,000), were used. PVP samples of PVP25K (MW= ca. 35,000), PVP30K (ca. 40,000), and PVP90K (ca. 360,000) were used. Poly(vinyl alcohol), PVA1K (MW= 900–1,100), was a completely saponificated type (96.0%). HPAA, PEG, and PVA samples were purchased from Wako Pure Chemical Ind. Ltd. (Osaka) except PEG8K. PEG8K was obtained from MP Biochemicals, Inc., Solon, OH, USA. The water used for the sample preparation was purified by a Milli-Q reagent grade system (Advantage A10, Millipore Co., Bedford, MA, USA).

Preparation of the colloidal suspensions of polymer complexes

Colloidal sample suspensions were prepared in a vial where water was added first, then stock solution of HPAA and the stock solution of the neutral polymer were poured into the vial slowly using the disposable serological pipettes (1, 5, and 10 ml, Corning Lab. Sci., Co., New York, NY, USA). Finally, up-and-down mixing of the mixtures was made gently five to seven times. Colloidal suspensions were formed immediately by the mixing.

Observation of the dissipative structures

Of the sample suspension, 0.1 ml aliquot was carefully and gently placed onto a micro cover glass (30×30 mm, No. 1, thickness from 0.12 to 0.17 mm, Matsunami Glass, Kishiwada, Osaka, Japan) set in a plastic dish (type NH-52, 52 mm in diameter, 8 mm in depth, As One Co., Tokyo, Japan). The cover glass was used without further rinse. Four milliliters of the suspension was set on a medium-sized watch glass (70 mm, TOP Co., Tokyo, Japan). Five milliliters of the suspension was placed into a medium-sized Petri glass dish (42 mm in inner diameter and 15 mm in height, code 305-02, TOP Co.). The disposable serological pipettes (1 and 10 ml, Corning Lab. Sci., Co.) were used for the placement of the suspension in the substrates. The patterns during the course of dryness were observed for the solutions on a desk covered with a black plastic sheet. The room temperature was regulated at 24°C. Humidity of the room was not regulated and was between 40% and 52%.

Macroscopic patterns were observed on a Canon EOS10D digital camera with a macro-lens (EF 50 mm, f= 2.5) plus a life-size converter EF or a zoom-lens (Canon, EF28-70 mm, 1:2.8) on a cover glass and without the life-size converter in a medium glass dish or a medium watch glass, respectively. Microscopic drying patterns were observed with a metallurgical microscope (PME-3, Olympus Co., Tokyo, Japan). Thickness profiles of the dried films on a cover glass were measured on a laser 3D profile microscope (type VK-8500, Keyence Co., Osaka, Japan).

DLS and ELS measurements

The dynamic light-scattering (DLS) measurements were made on a DLS-7000 spectrophotometer (Otsuka Electron-

ics, Osaka, Japan) at 25±0.02°C. The sample of 5 ml was set in a Pyrex tube cell (12 mm outside diameter and 130 mm long). Data analysis was made with the cumulant analysis. Histogram methods including the nonnegative least square and the Marquadt analyses were also made for discussing the size distribution. The zeta-potential measurements were made on an electrophoresis light-scattering (ELS) spectrophotometer (LEZA-6000, Otsuka Electronics). The reproducibility of the ζ-potential was within 5%.

Results and discussion

Characterization of colloidal particles of polymer complexes

The hydrogen-bonding complexation reaction between HPAA and PEG, for example, is shown in Eq. 1 [57, 58].

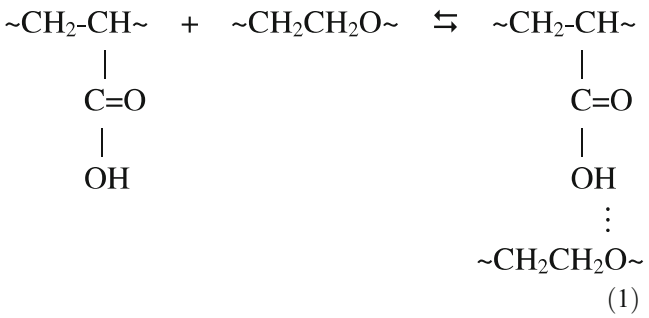

(1)

The hydrogen bonding (shown by dotted line) is formed between hydrogen of carboxylic acid group of HPAA and oxygen of main chain of PEG (or oxygen of pyrrolidone group of PVP). Dissociation of the carboxylic acid groups of HPAA is inhibited by the hydrogen bonding. Then, the concentrations of both hydronium cations and carboxylic anions decrease by the complexation following the equilibrium shown in Eq. 2.

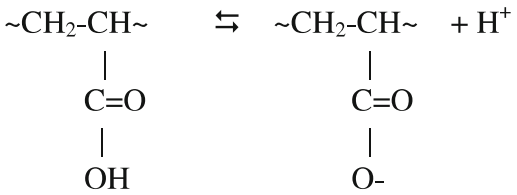

(2)

Potentiometric and conductometric measurements of the polymer complexation have been made [57–59, 69], and the kinetic analysis between HPAA and PVP has been made using the conductance stopped-flow technique [69].

In our experiments, the stable colloidal suspensions were obtained in the mixtures HPAA25K (0.05 monoM)+*X* (0.05 monoM), where *X* is PEG0.2K, PEG1K, PEG2K, PEG4K, PEG8K, PEG20K, PEG25K, or PVP30K. However, the sticky aggregates of the complexes were obtained instead of the colloidal dispersions, when *X* is PEG500K, PEG2000K, PEG3500K, or PVP90K. The critical molecular weights of the neutral polymers between the colloidal and aggregate state are located in between PEG20K and PEG500K, and PVP30K and PVP90K, respectively. It should be noted here that the polymer complex mixtures of HPAA0.64K (0.001–0.01 monoM)+PVP30K (0.001–0.01 monoM) were transparent liquid state and did not show any colloidal suspensions [69]. Furthermore, mixture HPAA25K (0.05 monoM)+PVA1K (0.05 monoM) were transparent liquid instead of colloidal suspension. Thus, with increase of the molecular weight of the polymer components, the complexes showed transparent solution, stable colloidal dispersion, and then the sticky aggregates.

Colloidal size, size distribution, and zeta-potential of the polymer complexes HPAA25K+PEG20K and HPAA25K+PVP25K are compiled in Table 1. These values were evaluated by DLS and ELS measurements. The size information supports that the complex formation forces of HPAA25K with PEG20K is weak compared with PVP25K, since colloidal size of the former complex is smaller than the latter. Zeta-potential of the complexes were negative, which was originated from the carboxylic acid groups of HPAA undoubtedly.

Drying dissipative patterns of HPAA, PEG, and PVP in aqueous solution

Figure 1 shows the change of the dissipative patterns during the course of dryness of the single component solutions of HPAA25K (a–d), PEG20K (e–h), and PVP25K (i–l) on a cover glass, respectively. The solutions

Table 1 Size and zeta-potential data of colloidal suspensions of HPAA25K+PEG20K and HPAA25K+PVP25K from dynamic light-scattering and electrophoresis light-scattering measurements

Suspension	Mean size (nm)	Size distribution (nm)		Zeta-potential (mV)
		First peak	Second peak	
HPAA25K+PEG20K[a]	42.7±0.3	53.9±10	5.1±0.7	−36.9
HPAA25K+PVP25K[b]	278±0.15	281±50	4.3±0.6	−38.6

[a] [HPAA25K]=[PEG20K]=0.025 monoM

[b] [HPAA25K]=[PVP25K]=0.05 monoM

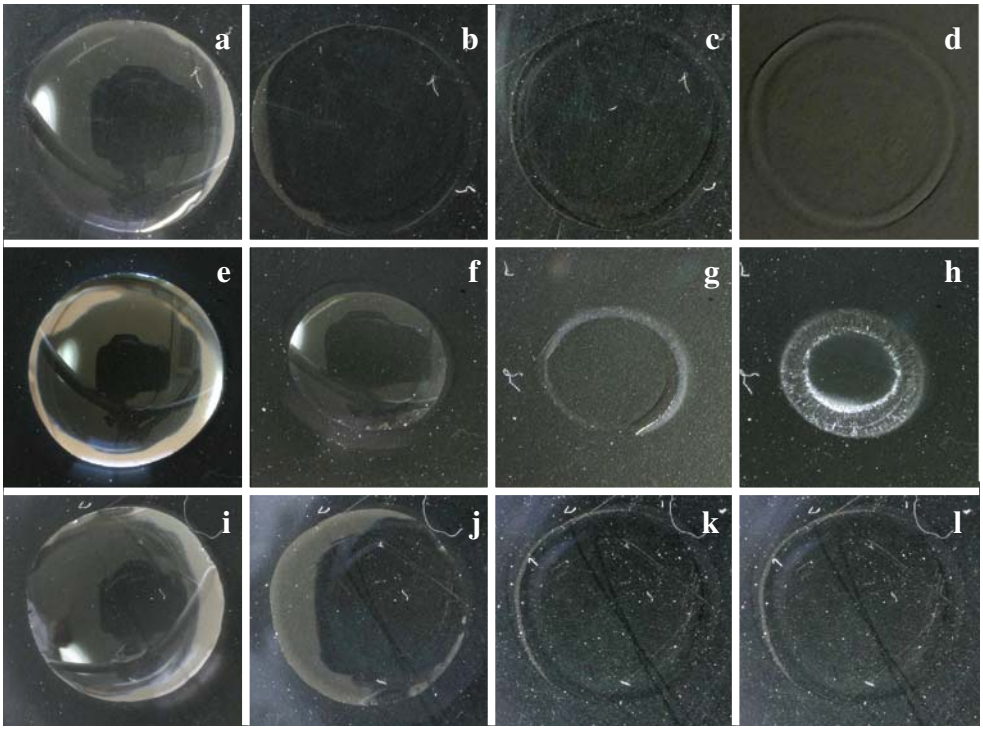

Fig. 1 Macroscopic dissipative patterns during the course of dryness of HPAA25K (**a**–**d**), PEG20K (**e**–**h**), and PVP25K (**i**–**l**) on a cover glass at 24 °C; 0.1 ml, 0.1 monoM: **a** 35 m after setting, **b** 3 h 5 m, **c** 7 h 20 m, **d** 7 h 20 m (on a white board), **e** 40 m after setting, **f** 3 h 50 m, **g** 4 h 35 m, **h** 5 h 25 m, **i** 35 m after setting, **j** 3 h 5 m, **k** 7 h 20 m, **l** 7 h 20 m (on a white board)

of HPAA25K were difficult to dry up completely and kept liquid state in the conditions of the room temperature and humidity. The clearcut pictures of liquid phase drying patterns were not taken as shown in Fig. 1d. Here, the scratches of the black plastic plates, which have not been observed in usual cases, were recognized clearly. The final drying patterns of HPAA250K were also liquid state (or transparent solid film), though the pictures showing this were omitted. The microscopic patterns of HPAA25K and HPAA 250K were not observed except showing the broad ring at the outside edge. It should be mentioned here that distinction between the liquid and solid states of the final film was difficult from the macroscopic and microscopic observation.

For PEG0.2K, the final patterns were liquid state at any concentrations. For PEG1K and PEG2K, the final patterns were liquid and coexistence of liquid and solid at low and high polymer concentrations, respectively. The liquid-state areas coexisted with the solid pattern areas at 0.003 monoM even for PEG4K and PEG8K. The solid-state drying patterns were, however, observed at high concentrations. From PEG20K to PEG3500K, solid drying patterns were observed with HPAA25K at any concentrations and areas of the dried film. Thus, the broad ring patterns were observed clearly irrespective of the liquid or solid states.

The macroscopic final drying patterns of PVP30K and PVP90K were liquid-like or transparent solid-like irrespective of the observation cells used (a cover glass, a watch glass, or a Petri dish). The microscopic drying patterns of PVP25K, PVP30K, and PVP90K were not observed by microscopy, except broad ring patterns. The water-soluble polymers HPAA and PVP have a large number of water-affinitive groups, i.e., carboxylic acid and tertiary amine groups, respectively. The drying processes of PVA1K solution (0.001 to 0.1 monoM)

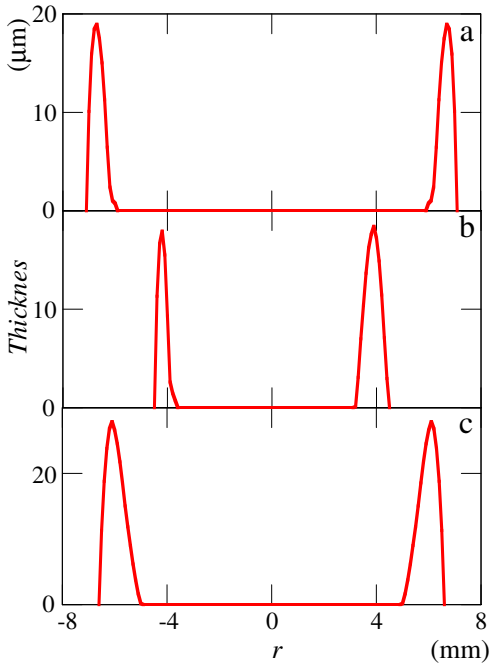

Fig. 2 Thickness profiles of dried film of HPAA25K (**a**), PEG20K (**b**), and PVP25K (**c**) on a cover glass at 24 °C; 0.1 ml and 0.1 monoM

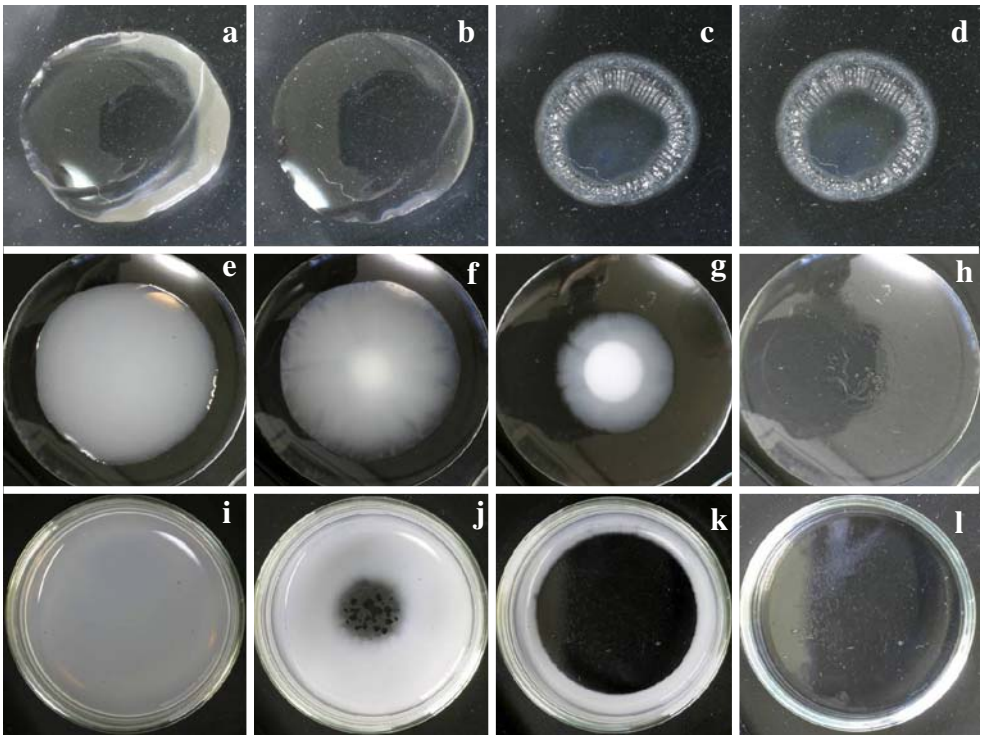

Fig. 3 Macroscopic dissipative patterns during the course of dryness of HPAA25K (0.05 monoM)+PEG8K (0.05 monoM) mixtures during the course of dryness on a cover glass (**a**–**d**), a watch glass (**e**–**h**), and a Petri glass dish (**i**–**l**) at 24° C; 0.1 ml: **a** 35 m after setting, **b** 2 h, **c** 4 h 10 m, **d** 6 h 20 m, **e** 5 m after setting, **f** 5 h 35 m, **g** 17 h 40 m, **h** 26 h 35 m, **i** 15 m after setting, **j** 64 h 20 m, **k** 71 h 30 m, **l** 87 h 50 m

were observed on a cover glass. The final films were dried completely, and the broad ring areas were transparent solid film especially at 0.03 and 0.1 monoM.

The thickness profiles of the dried film are shown in Fig. 2. All the polymers were accumulated at the broad ring areas at the outside edge of the film even in the liquid phases. Origin of the broad ring formations is, undoubtedly, due to the convectional flow of colloidal particles from the central area toward the outside edge in the bottom layers of the liquids in the convectional processes. It should be noted here that the broad-ring patterns were observed for most of the solutions and suspensions [1, 2].

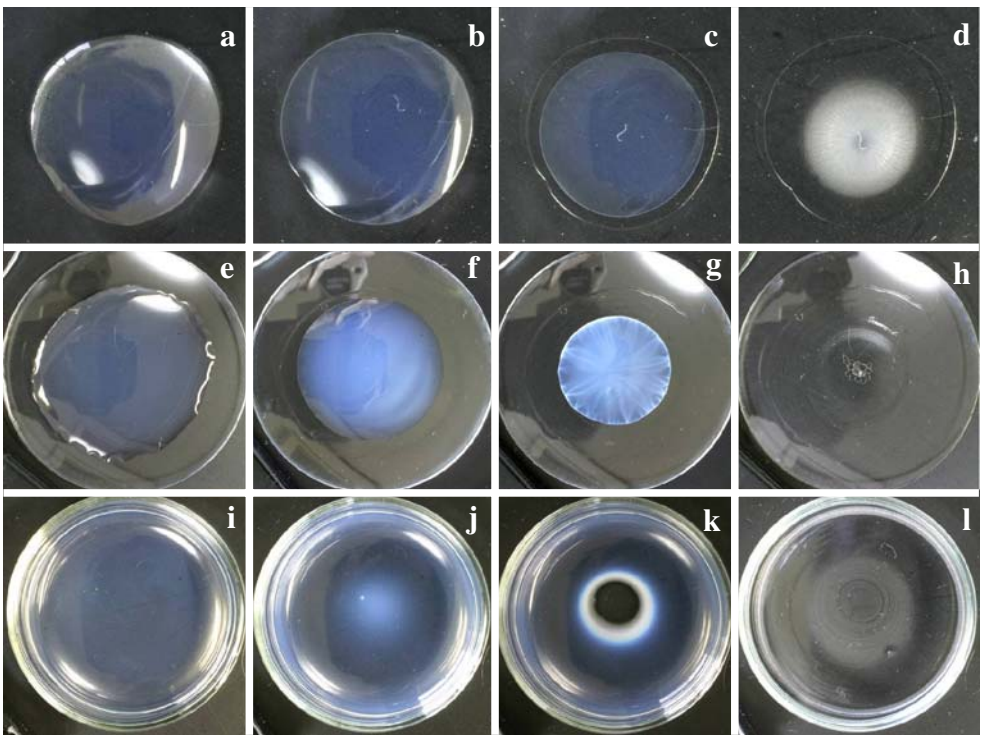

Fig. 4 Macroscopic patterns during the course of dryness of HPAA25K (0.05 monoM)+ PVP25K (0.05 monoM) mixtures during the course of dryness on a cover glass (**a**–**d**), a watch glass (**e**–**h**), and a Petri dish (**i**–**l**) at 24°C; 0.1 ml: **a** 10 m after setting, **b** 1 h 40 m, **c** 2 h 45 m, **d** 6 h 35 m, **e** 5 m after setting, **f** 14 h 45 m, **g** 20 m, **h** 26 h 35 m, **i** 15 m after setting, **j** 67 h 10 m, **k** 67 h 50 m, **l** 87 h 50 m

Macroscopic patterns of HPAA+PEG and HPAA+PVP complexes

Figure 3 shows the change in patterns during the course of dryness of HPAA25K+PEG8K complexes on a cover glass (a–d), a watch glass (e–h), and a Petri glass dish (i–l), respectively. These complex mixtures showed quite stable colloidal suspensions. In a watch glass, the spoke-like convectional patterns, i.e., Terada cell, were observed with the naked eye (see Fig. 3f). It should be noted that the Terada cell was dynamic, and the association and separation of the spoke lines (clustering) repeated with time. The broad rings were always observed at the outside areas of the dried film irrespective of the substrates used among a cover glass, a watch glass, and a Petri dish. Drying processes of the mixtures HPAA25K+PEG20K, HPA25K+PEG4K, HPAA25K+PEG2K, HPAA25K+PEG1K, and HPAA25K+PEG0.2K were also studied on a cover glass, a watch glass, and a Petri glass dish. The macroscopic drying patterns were quite similar to those of HPAA25K+PEG8K shown in Fig. 3 except the complex between HPAA25K and PEG0.2K, where the final films were transparent and liquid-like.

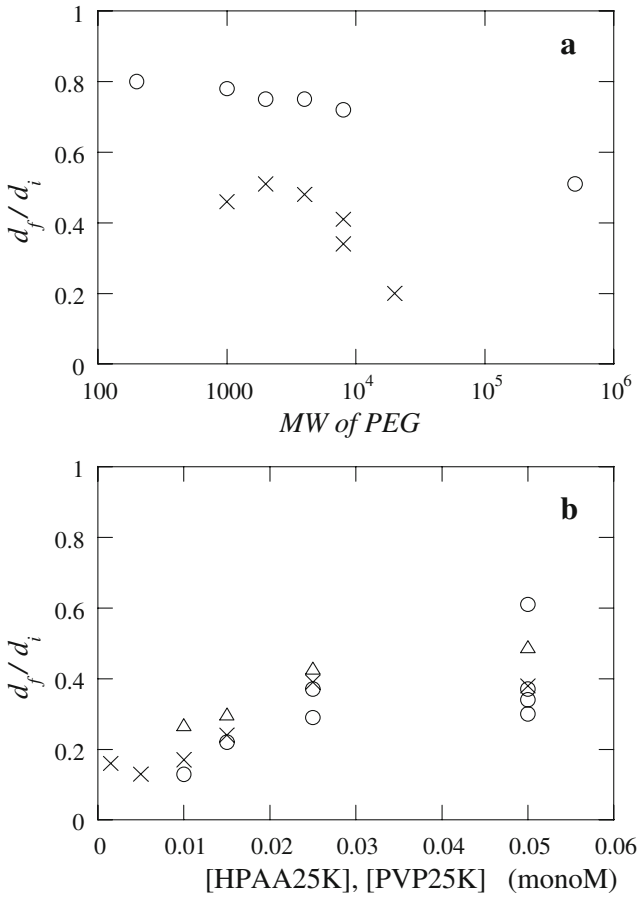

Fig. 5 **a** Plots of df/di of HPAA25K+PEG as a function of molecular weight of PEG on a cover glass (*circles*) and a watch glass (*X*) at 24°C. [HPAA25K]=[PEG]=0.05 monoM. **b** Plots of df/di of HPAA25K+PVP25K as a function of polymer concentration on a cover glass (*circles*), a watch glass (*X*), and a glass dish (*triangles*)

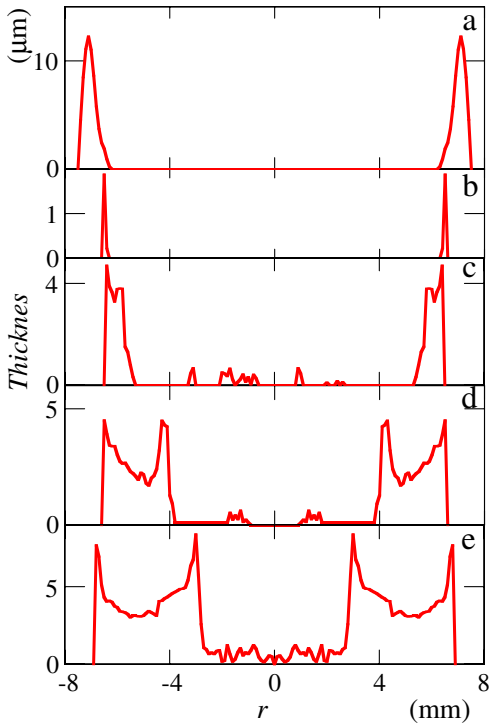

Fig. 6 Thickness profiles of dried film of HPAA25K+PEG20K (**a**) and HPAA25K+PVP25K (**b**–**e**) on a cover glass at 24°C; 0.1 ml: **a** [HPAA25K]=[PVP25K]=0.05 monoM, **b** [HPAA25K]=[PEG20K]=0.0015 monoM, **c** 0.01 monoM, **d** 0.025 monoM, **e** 0.05 monoM

Figure 4 shows the macroscopic patterns of HPAA25K+PVP25K. In general, when the molecular weights of each component are large enough, the affinitive forces between the polymers came to be strong enough to form the colloidal suspensions. It should be noted here that the colloidal suspensions of HPAA25K+PVP25K showed bluish colors, and the suspensions kept bluish during the course of dryness until complete dryness, where the dried films were bluish white and/or transparent in part as shown in Fig.4d, h, and l. The bluish colors support strongly that the suspensions formed colloidal crystal and higher in the monodispersity of the colloidal complexes of HPAA25K and PVP25K. Table 1 also supports that the size 278 nm and higher in the monodispersity of the HPAA25K+PVP25K colloids (±0.15 nm) are quite appropriate for the formation of colloidal crystal [70, 71]. The beautiful color rings appeared especially in a Petri dish, though the yellow and pink colors are not recognized so clearly in Fig. 4k. The spoke-like convectional patterns were observed clearly in a watch glass (see Fig. 4g). The clustering of the spoke lines were also observed in the several places. It should be noted that the convectional patterns have been observed only for the suspensions of non-spherical particles, aqueous

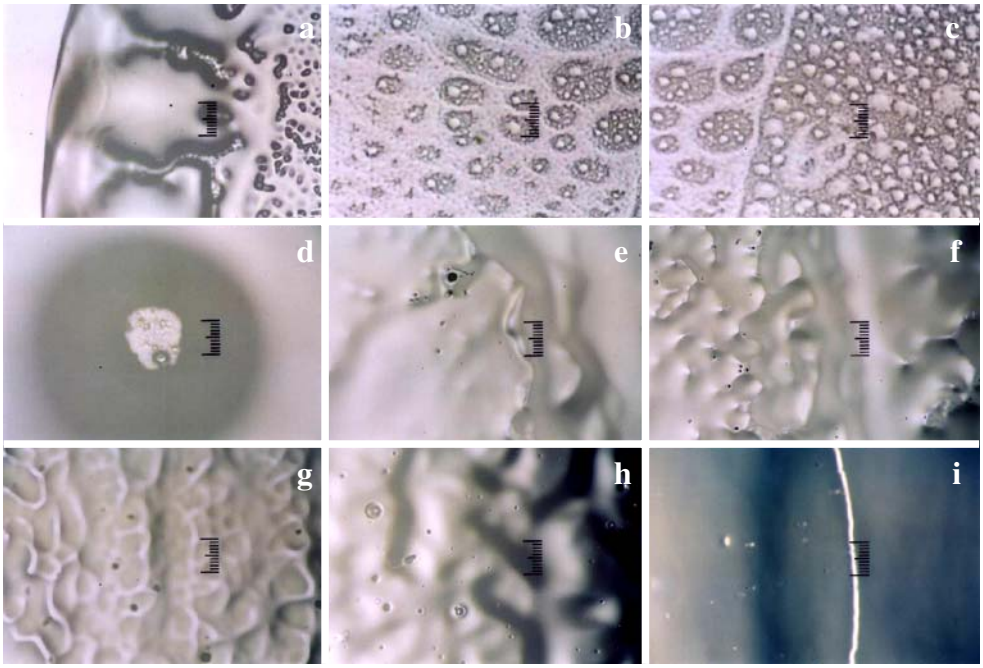

Fig. 7 Microscopic drying patterns of HPAA25K (0.05 monoM)+PEG8K (0.05 monoM) on a cover glass at 24°C. **a**–**c** From the left edge to the center, 6 h 35 m after setting, 0.1 ml, full scale=200 μm at 24 °C. **d**–**i** From the center to the right edge in a watch glass, 71 h 30 m after setting, 4 ml, full scale=200 μm

colloidal crystals of spherical particles [14–16], and 100% ethanol suspensions of spheres [9]. Drying processes of HPAA25K+PVP30K systems were also studied in this work on a cover glass, a watch glass, and a Petri dish. Colloidal crystals were also formed. The macroscopic drying patterns were quite similar to those of HPAA25K+PVP25K shown in Fig. 4, for example.

Figure 5a shows the values of the broad ring size of the dried films (df) divided by the initial size of the suspension (di) of HPAA25K+PEG as a function of molecular weight of PEG (MW) on a cover glass (*O*) and a watch glass (*X*). Size of the broad ring decreased as MW increased irrespective of the observation cells. This supports that the size of the complex particles increases and the particle

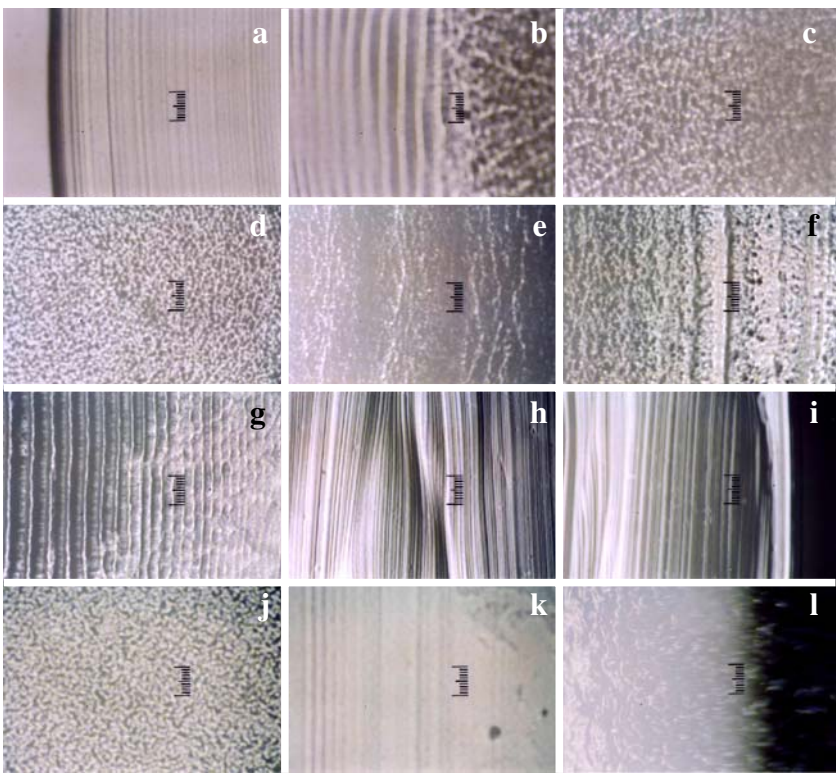

Fig. 8 Microscopic drying patterns of HPAA25K (0.05 monoM)+PVP25K (0.05 monoM) at 24°C. **a**–**c** From the left edge to center on a cover glass, 7 h 15 m after setting, 0.1 ml, full scale=100 μm. **d**–**i** From the center to the right edge in a watch glass, 29 h 5 m after setting, 4 ml, full scale=200 μm in a glass dish at 24°C. **j**–**f** From the center to the right edge in a Petri glass dish, 87 h 50 m after setting, 5 ml, full scale=100 μm

number decreases in the suspension as *MW* increases. Decrease in the particle number should result in decrease of the broad ring size, since the broad ring size decreases until the nearest neighbored particle–particle interactions are strong enough to form the inter-particle structures [55, 56]. It should be recalled that the change in the size of the broad rings does not support the pinning effect of the contact line proposed by Deegan et al. [21]. Figure 5b shows the df/di values plotted against the concentration of the polymer in the complexes HPAA25K+PVP25K. The broad ring size increased sharply as the polymer concentration increased. This observation is quite understandable because the particle–particle interactions increase sharply with increasing concentration.

Figure 6 shows the thickness profiles of the dried films of the complexes HPAA25K+PEG20K (a) and HPAA25K+PVP25K (b–e) on a cover glass. Concentrations of polymer components of a are 0.05 monoM, and those of b to e increase from 0.0015 to 0.05 monoM. The profiles shown in a are typical ones, and most of the particles are accumulated in the broad ring area even at high polymer concentrations. This is due to the fact that the particle size of the complexes HPAA25K+PEG20K is small enough, and the fast convectional flows of particles take place during the drying processes. On the other hand, the thickness profiles of HPAA25K+PVP25K were much complex especially at high polymer concentrations, though the broad ring patterns were clear. As discussed above, the complex suspensions of HPAA25K+PVP25K is *colloidal crystal* state, and the cooperated long-range inter-particle electrostatic repulsive interactions prevail in the whole suspension during the convectional and sedimentary processes. The convectional flow of each particle must be retarded strongly in the network of colloidal crystals. The profiles shown in c to e indicate the formation of the multiple-type broad ring formation.

Microscopic patterns of HPAA+PEG and HPAA+PVP complexes

Figure 7 shows the typical microscopic patterns of HPAA25K+PEG8K complex on a cover glass (a–c) and on a watch glass (d–i). The concentrations of each polymer components were 0.05 monoM in the initial mixture. On a cover glass, the spoke-like microscopic patterns are clear in the broad ring area (see Fig. 7a). Furthermore, many granules composed of the colloidal particles and further group formation of the granules are observed in the middle and central area of the dried film. This observation supports that the complexes are rather small, and affinitive inter-particle interactions are strong on a cover glass substrate. On a watch glass, microscopic pictures were not so clear, which is due to the fact that the film was not dried completely, and liquid-state parts remained on the substrate. Furthermore, netted patterns were observed (see Fig. 7g). Microscopic patterns of HPAA25K+PEG20K were similar to those of HPAA25K (0.05 monoM)+PEG4K (0.05 monoM), HPAA25K+PEG2K, and HPAA25K+PEG1K, which showed the regularly crossed patterns of fine multiple rings and the spoke lines in the area of the broad ring.

The microscopic patterns of HPAA25K+PVP25K shown in Fig. 8 on a cover glass (a–c) were quite typical ones compared with the HPAA25K+PEG8K systems. The multiple fine-ring structures are clear on the three kinds of observation cells. Furthermore, crossed ordered structures of the fine rings and the fine spoke lines were observed on all the substrates especially on a watch glass (see Fig. 8g). It is interesting to note that the whole areas of the dried film of HPAA25K+PVP25K are the state of the *freeze-state* colloidal crystal. However, the microstructures differ as a function of the distance from the center of the dried film. It should be mentioned here that the microscopic drying patterns of HPAA25K+PVP30K on a cover glass, a watch glass, and a Petri dish were similar to those of HPAA25K+PVP25K shown in Fig. 8.

Concluding remarks

The stable colloidal dispersions of polymer complexes of HPAA+PEG and HPAA+PVP were obtained in the restricted conditions of the molecular weight of each polymer. Especially, suspensions of HPAA25K+PVP25K were monodispersed in the particle size distribution and showed *colloidal crystal*. Convectional and sedimentary patterns were observed clearly for the colloidal crystals. Size of the macroscopic drying broad rings of HPAA25K+PEG decreased when molecular weight of PEG increased. Furthermore, the size increased sharply as polymer concentration increased in the complexes between HPAA25K and PVP25K. Characteristic microscopic patterns were also observed in the polymer complexes. Importance of the convectional flow in the processes of the drying patterns was understood in this study.

Acknowledgments Financial supports from the Ministry of Education, Culture, Sports, Science, and Technology, Japan, and Japan Society for the Promotion of Science are greatly acknowledged for Grants-in-Aid for Exploratory Research (17655046 to T.O.) and Scientific Research (B; 18350057 to T.O. and 19350110 to A.T.). Research grant from Rex Co., Tokyo, Japan, to T.O. is also appreciated deeply.

References

1. Okubo T (2006) In: Stoylov SP, Stoimenova MV (eds) Molecular and colloidal electro-optics. Taylor & Francis, New York, p 573

2. Okubo T (2008) In: Nagarajan R, Hatton TA (eds) Nanoparticles: syntheses, stabilization, passivation and functionalization. ACS, Washington DC, p 256
3. Gribbin G (1999) Almost everyone's guide to science. The universe, life and everything. Yale University Press, New Haven
4. Ball P (1999) The self-made tapestry. Pattern formation in nature. Oxford University Press, Oxford
5. Terada T, Yamamoto R, Watanabe T (1934) Sci Papers Inst Phys Chem Res Jpn 27:173 Proc Imper Acad Tokyo 10:10
6. Terada T, Yamamoto R, Watanabe T (1934) Sci Papers Inst Phys Chem Res Jpn 27:75
7. Nakaya U (1947) Memoirs of Torahiko Terada (Japanese). Kobunsya, Tokyo
8. Okubo T, Kimura H, Kimura T, Hayakawa F, Shibata T, Kimura K (2005) Colloid Polym Sci 283:1
9. Okubo T (2006) Colloid Polym Sci 285:225
10. Okubo T (2009) Colloid Polym Sci 287:167
11. Deegan RD, Bakajin O, Dupont TF, Huber G, Nagel SR, Witten TA (1997) Nature 389:827
12. Okubo T, Okamoto J, Tsuchida A (2009) Colloid Polym Sci 287:351
13. Okubo T (2009) Colloid Polym Sci 287:645
14. Okubo T, Okamoto J, Tsuchida A (2008) Colloid Polym Sci 286:1123
15. Okubo T (2008) Colloid Polym Sci 286:1307
16. Okubo T (2008) Colloid Polym Sci 286:1527
17. Palmer HJ (1976) J Fluid Mech 75:487
18. Anderson DM, Davis SH (1995) Phys Fluids 7:248
19. Pouth AF, Russel WB (1998) AIChE J 44:2088
20. Burelbach JP, Bankoff SG (1998) J Fluid Mech 195:463
21. Deegan RD, Bakajin O, Dupont TF, Huber G, Nagel SR, Witten TA (2000) Phys Rev E 62:756
22. Fischer BJ (2002) Langmuir 18:60
23. Okubo T (2006) Colloid Polym Sci 284:1191
24. Okubo T (2006) Colloid Polym Sci 284:1395
25. Okubo T, Okamoto J, Tsuchida A (2007) Colloid Polym Sci 285:967
26. Okubo T (2007) Colloid Polym Sci 285:1495
27. Okubo T, Okamoto J, Tsuchida A (2008) Colloid Polym Sci 286:385
28. Okubo T, Okamoto J, Tsuchida A (2008) Colloid Polym Sci 286:941
29. Yamaguchi T, Kimura K, Tsuchida A, Okubo T, Matsumoto M (2005) Colloid Polym Sci 283:1123
30. Okubo T (2006) Colloid Polym Sci 285:331
31. Vanderhoff JW (1973) J Polym Sci Polym Symp 41:155
32. Nicolis G, Prigogine I (1977) Self-organization in non-equilibrium systems. Wiley, New York
33. Ohara PC, Heath JR, Gelbart WM (1997) Angew Chem 109:1120
34. Maenosono S, Dushkin CD, Saita S, Yamaguchi Y (1999) Langmuir 15:957
35. Nikoobakht B, Wang ZL, El-Sayed MA (2000) J Phys Chem 104:8635
36. Ung T, Litz-Marzan LM, Mulvaney P (2001) J Phys Chem B 105:3441
37. Okubo T, Okuda S, Kimura H (2002) Colloid Polym Sci 280:454
38. Okubo T, Kimura K, Kimura H (2002) Colloid Polym Sci 280:1001
39. Okubo T, Kanayama S, Kimura K (2004) Colloid Polym Sci 282:486
40. Okubo T, Yamada T, Kimura K, Tsuchida A (2005) Colloid Polym Sci 283:1007
41. Okubo T, Nozawa M, Tsuchida A (2007) Colloid Polym Sci 285:827
42. Okubo T, Kimura K, Tsuchida A (2007) Colloids Surf B Biointerfaces 56:201
43. Okubo T, Nakagawa N, Tsuchida A (2007) Colloid Polym Sci 285:1247
44. Okubo T (2008) In: Nagarajan R, Hatton TA (eds) Nanoparticles: syntheses, stabilization, passivation and functionalization. ACS, Washington DC
45. Okubo T, Kimura K, Tsuchida A (2008) Colloid Polym Sci 286:621
46. Okubo T, Otake A, Tsuchida A (2009) Colloid Polym Sci 287:1435
47. Okubo T, Kanayama S, Ogawa H, Hibino M, Kimura K (2004) Colloid Polym Sci 282:230
48. Okubo T, Onoshima D, Tsuchida A (2007) Colloid Polym Sci 285:999
49. Shimomura M, Sawadaishi T (2001) Curr Opin Colloid Interface Sci 6:11
50. Okubo T, Yamada T, Kimura K, Tsuchida A (2006) Colloid Polym Sci 284:396
51. Kimura K, Kanayama S, Tsuchida A, Okubo T (2005) Colloid Polym Sci 283:898
52. Okubo T, Shinoda C, Kimura K, Tsuchida A (2005) Langmuir 21:9889
53. Okubo T, Itoh E, Tsuchida A, Kokufuta E (2006) Colloid Polym Sci 285:339
54. Okubo T, Yokota N, Tsuchida A (2007) Colloid Polym Sci 285:1257
55. Okubo T, Okamoto J, Takahashi S, Tsuchida A (2009) Colloid Polym Sci 287:933
56. Okubo T, Hagiwara A, Kitano H, Okamoto J, Takahashi S, Tsuchida A (2009) Colloid Polym Sci 287:1155
57. Osada Y, Saito M (1976) J Polym Sci Letter 14:129
58. Osada Y (1979) J Polym Sci Part A Polym Chem 17:3485
59. Tsuchida E, Abe K (1982) Adv Polym Sci 45:1
60. Oyama HT, Tang WT, Frank CW (1986) Am Chem Soc Polym Div Polym Chem 27:248
61. Zhang X, Takegoshi K, Hikichi K (1991) Polym J 23:87
62. Paladhi R, Singh RP (1994) J Appl Polym Sci 51:1559
63. Philoppova OE, Starodubtzev SG (1995) J Macromol Sci Chem A32:1893
64. Lee YM, Kim SH, Cho CS (1996) J Appl Polym Sci 62:301
65. Doseva V, Shenkov S, Baranovsky VU (1997) Polymer 38:1339
66. Polacco G, Petarca MG, Peretti A (2000) Eur Polym J 36:254
67. Murkeeva ZS, Mun GA, Duborazov AV, Khutoryaskiy VV (2005) Macromol Biosci 5:424
68. Nugent MJD, Higginbothan CL (2006) J Mater Sci 41:2393
69. Okubo T (1980) Biophys Chem 11:425
70. Okubo T (1988) Acc Chem Res 21:281
71. Okubo T (1994) In: Schmitz KS (ed) Macro-ion characterization. From dilute solutions to complex fluids. ACS Book, Washington DC, p 364